

See discussions, stats, and author profiles for this publication at: <https://www.researchgate.net/publication/389531054>

Voltage-controlled surface plasmon in a flexoelectric nematic liquid crystal cell

Article in *Liquid Crystals* · March 2025

DOI: 10.1080/02678292.2025.2470121

CITATIONS
0

READS
21

2 authors, including:



Ivan I Yakovkin
Taras Shevchenko National University of Kyiv

41 PUBLICATIONS 69 CITATIONS

[SEE PROFILE](#)

ARTICLE TEMPLATE

Voltage-controlled surface plasmon in a flexoelectric nematic liquid crystal cell

Ivan Yakovkin and Mykhailo Ledney

Physics Faculty, Taras Shevchenko National University of Kyiv, Kyiv 01601, Ukraine

ARTICLE HISTORY

Compiled December 16, 2024

ABSTRACT

The orientational instability of the director field in a homeotropically oriented flexoelectric nematic liquid crystal (NLC) cell under an electric field is theoretically analyzed, focusing on its impact on surface plasmon polariton (SPP) propagation. The electro-induced transition of the director from the homeotropic to the planar state, and vice versa, may involve up to two hysteresis loops, with the number and parameters of these loops determined by the NLC cell parameters, particularly the flexoelectric ones. It is shown that orientational instability of the initial homeotropic state has a threshold only if the flexoelectric coefficient e_3 is zero. Increasing the magnitude of e_3 and adjusting e_1 based on the sign of e_3 lowers the threshold voltages for director reorientation compared to non-flexoelectric NLCs. The propagation of SPPs in a metal–polymer–NLC system is theoretically studied, revealing the influence of applied voltage and NLC parameters on the SPP effective refractive index. An increase in the absolute value of e_3 narrows the voltage range for tuning the effective refractive index and shifts the voltage range to lower voltages. Increasing the value of e_1 shifts the voltage range towards higher voltages if e_3 is negative, and towards lower voltages otherwise.

KEYWORDS

nematic liquid crystal; flexopolarization; orientational instability; hysteresis of the orientational transition; surface plasmon polariton; anchoring energy

1. Introduction

Intensive scientific research in the field of liquid crystal (LC) physics has led to their widespread practical applications, particularly in physics, medicine, and industry [1,2]. The use of LC cells as components of various electro-optical devices is associated with their relatively low cost and their unique electro- and magneto-optical properties [3–6]. These properties are closely related to the orientational ordering of the mesophase and significantly depend on the boundary conditions for the director on the confining surface of the cell [7–9]. Due to the long-range interactions between LC molecules, the influence of the surface extends into the volume of the LC sample, creating a certain orientational order within it [10–14]. This ordering can be relatively easily controlled thanks to the high sensitivity of LCs to external fields (electric, magnetic, or light) [15–20]. As a result, the optical properties of the entire LC cell can be non-invasively altered. This makes LC systems a promising tool for the effective and easy control of the propagation and transmission of electromagnetic signals.

As it turns out, orientational transitions induced by an external field in the volume of LCs, particularly nematic ones, can be accompanied by hysteresis, which manifests in bistability [21–24] and multistability [25,26] of the director field. Such features of orientational restructuring of nematic liquid crystals (NLCs) can occur in both a constant electric [27] and light [21,28,29] field. This expands the prospects of using NLC systems in the creation of highly efficient bistable displays, optical shutters, and the like. Modern laboratory and technological applications have

opened possibilities for effectively controlling the optical and spectral properties of photonic crystals [30,31], waveguides [32], and other applications by using NLC layers in them as control elements.

In the case of significant asymmetry of NLC molecules, the flexoelectric effect plays an important role in the interaction of the latter with the electric field [33,34]. This effect can significantly influence the characteristics of electro-induced orientational transitions, particularly the threshold voltage values and the dynamics of the reorientation of the director field [8]. In particular, in [35], it was shown that the use of flexoelectric NLC in an in-plane switching (IPS) configuration can lead to improvements in the energy efficiency of modern displays. A detailed study of the influence of flexopolarization in NLC cells of different configurations is especially important due to the possibility of enhancing/weakening the flexoelectric properties of NLC by adding special dopants to it [36].

Recently, LCs, particularly NLCs, has been widely used for dynamic control of the characteristics of plasmonic structures [37–41]. As is known, under certain conditions, surface plasmon polaritons (SPPs) can be excited at the metal – insulator interface. The increased sensitivity of the latter to small changes in the dielectric permittivity of the medium on one side, and the high sensitivity of NLC to the influence of external fields on the other, found a successful combination in a three-layer NLC – polymer layer – metal system. This structure allows for the control of the propagation characteristics of SPPs, particularly the value of its effective refractive index, by changing the orientation of NLC with an external field [42–47]. The ability to control the propagation characteristics of SPPs using NLCs has opened the way for the creation of spatial light modulators [48,49], spectral filters [50–52], light intensity modulators [53,54], gratings with controlled transmission coefficients [55], and more.

In this work, the influence of orientation instability of the director field in a homeotropic flexoelectric NLC cell induced by an external electric field on the characteristics of plasmon polariton propagation on the cell surface is theoretically investigated. The work is organized as follows. In section 2, the model is described, and the free energy of the NLC cell is formulated. In the approximation of planar deformations, equations for the director angle and boundary conditions for it are derived. Solutions are found in quadratures. Section 3 presents the results of numerical calculations of possible director orientation transitions in the volume of the NLC, in particular hysteresis transitions, with an increase/decrease in the applied potential difference. The values of the hysteresis parameters (threshold voltages, width, and amplitude) are established depending on the values of the NLC cell parameters, in particular, the flexoelectric coefficients. Section 4 investigates the influence of the NLC cell parameters on the number of hysteresis loops and their existence regions. In section 5, the propagation of SPP in a three-layer system NLC – polymer film – metal is theoretically considered. The value of the effective refractive index of the SPP is calculated depending on the voltage, the thickness of the polymer layer, and the parameters of the NLC layer, particularly the flexoelectric ones. Discussion of the results and brief conclusions are presented in section 6.

2. Free energy of the NLC and the equations for the director

Let us consider a plane-parallel cell of flexoelectric NLC, confined by the planes $z = 0$ and $z = L$, with an initial homeotropic orientation of the director along the Oz axis. The cell is in a constant electric field with the electric field vector \mathbf{E}_0 oriented along the Ox axis. The electric field is created by a constant potential difference U over the length d of the cell. The anchoring of the NLC with the surface at $z = L$ of the upper substrate is considered infinitely strong. The anchoring energy of the NLC with the surface at $z = 0$ of the lower substrate is finite and equals W .

The free energy of the NLC cell is written as

$$F = F_{el} + F_E + F_S, \quad (1)$$

$$F_{el} = \frac{1}{2} \int_V \left\{ K_1(\operatorname{div} \mathbf{n})^2 + K_2(\mathbf{n} \cdot \operatorname{rot} \mathbf{n})^2 + K_3[\mathbf{n} \times \operatorname{rot} \mathbf{n}]^2 \right\} dV,$$

$$F_E = \int_V \left(-\frac{1}{8\pi} \mathbf{E} \hat{\epsilon} \mathbf{E} - \mathbf{P} \mathbf{E} \right) dV,$$

$$F_S = -\frac{W}{2} \int_S (\mathbf{e} \mathbf{n})^2 dS, \quad W > 0.$$

Here, F_{el} is the elastic energy of the NLC, F_E represents the anisotropic and flexoelectric contributions to the free energy due to the interaction of the NLC with the electric field, and F_S is the interaction energy of the NLC with the surface at $z = 0$ of the lower substrate, written in the form of the Rapini potential [56], K_1, K_2, K_3 are the elastic constants, \mathbf{n} is the director, and \mathbf{E} is the electric field vector in the NLC volume. The tensor $\hat{\epsilon} = \epsilon_{\perp} \hat{\mathbf{1}} + \epsilon_a \mathbf{n} \otimes \mathbf{n}$ represents the static dielectric permittivity, where $\epsilon_a = \epsilon_{\parallel} - \epsilon_{\perp} > 0$ is the dielectric anisotropy. The flexoelectric polarization vector of the NLC is given by $\mathbf{P} = e_1 \mathbf{n} \operatorname{div} \mathbf{n} - e_3 [\mathbf{n} \times \operatorname{rot} \mathbf{n}]$, with e_1 and e_3 being the flexoelectric coefficients, and the vector $\mathbf{e} = (0, 0, 1)$ describes the axis of easy orientation of the NLC director at the surface $z = 0$.

In the considered geometric configuration of the initially uniform director field and the external electric field, the orientational instability of the director field can manifest both as a planar deformation and as a formation of a spatially periodic structure [57]. We will consider planar deformations of the NLC director field that lie in the xOz plane. The condition for the deformations of the latter type is $\epsilon_a K_2 / 4\pi(e_1 - e_3)^2 \geq 1$, as in [57]. Due to the homogeneity of the system in the direction of the Oy axis, the director in the volume of the NLC can be written as

$$\mathbf{n} = (\sin \theta, 0, \cos \theta), \quad (2)$$

where $\theta(z)$ is the angle of deviation of the director from its initial orientation along the Oz axis.

It is clear that the equation for the director must be considered in conjunction with the equations for the electric field in the NLC volume. Assuming the system is homogeneous in the direction of the Ox axis, the electric field vector in the NLC volume can be written as $\mathbf{E} = (E_x(z), 0, E_z(z))$. According to the equation $\operatorname{rot} \mathbf{E} = 0$, the E_x component of the vector \mathbf{E} is constant, and due to the boundary conditions of electrostatics, $E_x = U/d$. From the equation $\operatorname{div} \mathbf{D} = 0$, it follows that the z -component of the electric displacement vector $\mathbf{D} = \hat{\epsilon} \mathbf{E} + 4\pi \mathbf{P}$ is constant and equal to 0, according to the boundary conditions of electrostatics. From this, we find the expression for the z -component of the \mathbf{E} vector,

$$E_z = -\frac{1}{\epsilon_{zz}} \left(\epsilon_{xz} \frac{U}{d} + 4\pi P_z \right),$$

where ϵ_{xz} and ϵ_{zz} are the components of the tensor $\hat{\epsilon}$. Consequently, the free energy F per unit area of the cell surface (1) can be written as:

$$F = \int_0^L \left[\frac{1}{2} (K_1 \sin^2 \theta + K_3 \cos^2 \theta) \theta_z'^2 - \frac{\epsilon_{\parallel} \epsilon_{\perp} U^2}{8\pi d^2 \epsilon_{zz}} + \frac{U}{d} \left(\frac{\epsilon_{xz}}{\epsilon_{zz}} P_z - P_x \right) + 2\pi \frac{P_z^2}{\epsilon_{zz}} \right] dz - \frac{W}{2} \cos^2 \theta_0, \quad (3)$$

where $\theta_0 = \theta(z=0)$ is the angle of deviation of the director on the lower surface of the cell. Here, $P_x = (e_3 \cos^2 \theta - e_1 \sin^2 \theta) \theta'_z$, and $P_z = -(e_1 + e_3) \sin \theta \cos \theta \cdot \theta'_z$.

Through the minimization of the free energy (3) with respect to the angle θ , we obtain the equation

$$\begin{aligned} & (K_1 \sin^2 \theta + K_3 \cos^2 \theta) \theta''_{zz} + \frac{1}{2} (K_1 - K_3) \theta'^2_z \sin 2\theta + \frac{\epsilon_{\parallel} \epsilon_{\perp} U^2}{4\pi d^2} \frac{\epsilon_{xz}}{\epsilon_{zz}^2} + \\ & + \frac{\pi(e_1 + e_3)^2}{\epsilon_{zz}} \left(\theta'^2_z \sin 4\theta + \frac{\epsilon_{xz}}{\epsilon_{zz}} \theta'^2_z \sin^2 2\theta + \theta''_{zz} \sin^2 2\theta \right) = 0 \end{aligned} \quad (4)$$

and the corresponding boundary conditions

$$\begin{aligned} & \left[(K_1 \sin^2 \theta + K_3 \cos^2 \theta) \theta'_z + \frac{U}{\theta'_z d} \left(\frac{\epsilon_{xz}}{\epsilon_{zz}} P_z - P_x \right) + \right. \\ & \left. + \frac{\pi(e_1 + e_3)^2}{\epsilon_{zz}} \theta'_z \sin^2 2\theta - \frac{W}{2} \sin 2\theta \right]_{z=0} = 0, \end{aligned} \quad (5)$$

$$\theta|_{z=L} = 0, \quad (6)$$

where primes in the function $\theta(z)$ denote derivatives with respect to the argument z . The solution of equation (4), which satisfies the boundary conditions (5), (6), determines the NLC director field \mathbf{n} in the cell volume for a given potential difference U .

Integrating equation (4) with respect to the variable z , we obtain

$$\begin{aligned} & \left((K_1 \sin^2 \theta + K_3 \cos^2 \theta) (\epsilon_{\perp} + \epsilon_a \cos^2 \theta) + \pi(e_1 + e_3)^2 \sin^2 2\theta \right) \theta'^2_z = \\ & = \frac{\epsilon_{\parallel} \epsilon_{\perp} \epsilon_a U^2}{4\pi d^2} \frac{\cos^2 \theta - \cos^2 \theta_m}{\epsilon_{\perp} + \epsilon_a \cos^2 \theta_m}, \end{aligned} \quad (7)$$

where θ_m is the maximum value of the function $\theta(z)$ on the interval $0 \leq z \leq L$, which is reached at $z = z_m$. It is clear that the angle $\theta(z)$ of the director's deviation is a continuous and non-monotonic function of the coordinate z . Integrating equation (7) once more with respect to the variable z , taking into account the condition (6), we obtain the expression for determining the dependence $\theta(z)$:

$$\begin{aligned} z &= \chi(z_m - z) \frac{d}{U} \sqrt{\frac{4\pi(\epsilon_{\perp} + \epsilon_a \cos^2 \theta_m)}{\epsilon_{\parallel} \epsilon_{\perp} \epsilon_a}} \int_{\theta_0}^{\theta} S(\theta, \theta_m) d\theta + \\ & + \chi(z - z_m) \left(L - \frac{d}{U} \sqrt{\frac{4\pi(\epsilon_{\perp} + \epsilon_a \cos^2 \theta_m)}{\epsilon_{\parallel} \epsilon_{\perp} \epsilon_a}} \int_0^{\theta} S(\theta, \theta_m) d\theta \right), \end{aligned} \quad (8)$$

where the function $\chi(t) = 0$ if $t < 0$ and $\chi(t) = 1$ if $t > 0$, and the function $S(\theta, \theta_m)$ is given by the expression

$$S(\theta, \theta_m) = \sqrt{\frac{(K_1 \sin^2 \theta + K_3 \cos^2 \theta)(\epsilon_{\perp} + \epsilon_a \cos^2 \theta) + \pi(e_1 + e_3)^2 \sin^2 2\theta}{\cos^2 \theta - \cos^2 \theta_m}} d\theta. \quad (9)$$

Taking into account condition (5), the maximum director angle θ_m , the value of the coordinate z_m at which it is reached, and the director angle θ_0 at the surface $z = 0$ are determined

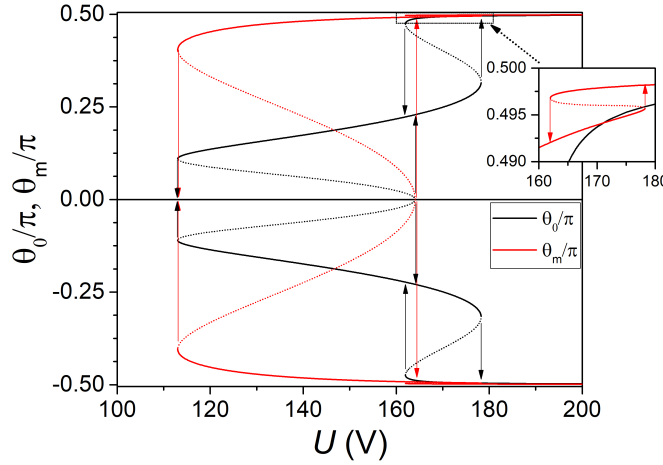


Figure 1. Dependencies of the maximum angle θ_m (—) and the surface director angle θ_0 (—) on the applied voltage U in the case of $e_1 = e_3 = 0$.

from the following system of equations:

$$z_m = \frac{d}{U} \sqrt{\frac{4\pi(\epsilon_{\perp} + \epsilon_a \cos^2 \theta_m)}{\epsilon_{\parallel} \epsilon_{\perp} \epsilon_a}} \int_{\theta_0}^{\theta_m} S(\theta, \theta_m) d\theta, \quad (10)$$

$$z_m = L - \frac{d}{U} \sqrt{\frac{4\pi(\epsilon_{\perp} + \epsilon_a \cos^2 \theta_m)}{\epsilon_{\parallel} \epsilon_{\perp} \epsilon_a}} \int_0^{\theta_m} S(\theta, \theta_m) d\theta, \quad (11)$$

$$\begin{aligned} \frac{\epsilon_{\parallel} \epsilon_{\perp} \epsilon_a U^2}{4\pi d^2} & \frac{[(K_1 \sin^2 \theta_0 + K_3 \cos^2 \theta_0)(\epsilon_{\perp} + \epsilon_a \cos^2 \theta_0) + \pi(e_1 + e_3)^2 \sin^2 2\theta_0](\cos^2 \theta_0 - \cos^2 \theta_m)}{(\epsilon_{\perp} + \epsilon_a \cos^2 \theta_0)^2 (\epsilon_{\perp} + \epsilon_a \cos^2 \theta_m)} = \\ & = \left[\frac{W}{2} \sin 2\theta_0 + \frac{U}{d} \left(\epsilon_a (e_1 + e_3) \frac{\sin^2 \theta_0 \cos^2 \theta_0}{\epsilon_{\perp} + \epsilon_a \cos^2 \theta_0} + e_1 \sin^2 \theta_0 + e_3 \cos^2 \theta_0 \right) \right]^2. \end{aligned} \quad (12)$$

The given system of equations (10)–(12) allows only numerical solutions.

3. Electrically induced reorientation of the director field

In Figs. 1 and 2, the dependencies of the maximum director deviation angle θ_m and the surface director angle θ_0 on the applied voltage U are shown for the dimensionless anchoring energy $w = WL/K_3 = 10$, both in the absence and presence of flexoelectric properties in the NLC, respectively. The calculations were performed using typical parameters of an NLC cell: $K_1 = 1.43 \cdot 10^{-6}$ dyn, $K_3 = 1.59 \cdot 10^{-6}$ dyn, $\epsilon_{\parallel} = 19.54$, $\epsilon_{\perp} = 5.17$ [43,58–60], $L = 12$ μm , and $d = 1$ mm. The unstable solutions of equations (10)–(12) are marked with dotted lines, and possible transitions between director states are indicated by arrows. It should be noted that the system of equations (10)–(12) has both sign-constant and sign-changing solutions with one or more nodes—similar to the classical problem of string oscillations. Although some of the sign-changing solutions are stable, the corresponding director states are not reached by

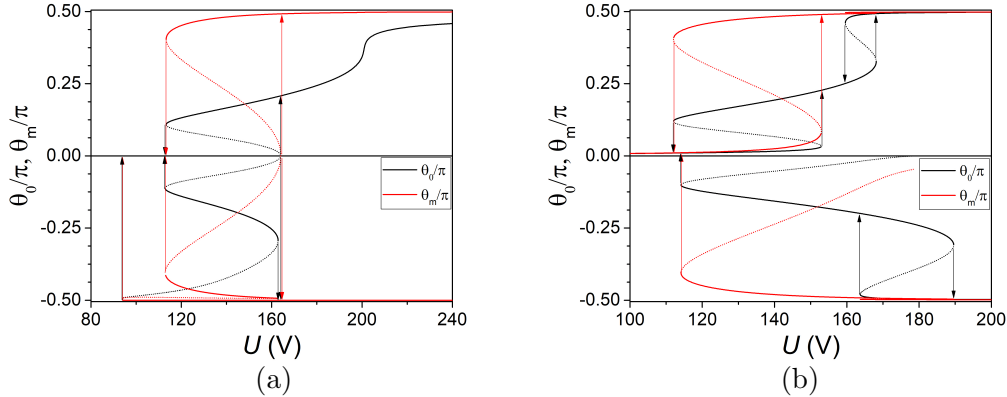


Figure 2. Dependencies of the maximum angle θ_m (—) and the surface director angle θ_0 (—) on the applied voltage U . a) $e_1 = 0.0001 \text{ dyn}^{1/2}$, $e_3 = 0$; b) $e_1 = 0$, $e_3 = -0.0001 \text{ dyn}^{1/2}$.

transitioning from the initial homeotropic configuration when varying the voltage. Therefore, we will not consider such solutions further. In general, as the voltage U increases from zero, the system undergoes an orientational transition from a uniformly oriented homeotropic state to a significantly non-uniform state, followed by a transition to a uniform planar state. This transition can be accompanied by one or two hysteresis loops (see Figs. 1, 2), specifically near the initial homeotropic and final planar states. In the presence of hysteresis, as the voltage U increases and reaches the threshold value U_{th} , the system abruptly transitions from a uniform or an almost uniform homeotropic state to a significantly non-uniform one, and subsequently from the non-uniform state to a planar state. When the voltage U decreases, the reverse transitions are also abrupt but occur at lower threshold values $U'_{th} < U_{th}$.

It should be noted that in the presence of flexopolarization in the NLC, the dependence of the director angle θ on the applied voltage U (see Fig. 2) differs significantly from the case where the NLC lacks flexoelectric properties (Fig. 1). In the latter case ($e_1 = e_3 = 0$), the dependencies $\theta(U)$ are symmetric with respect to the transformation $\theta \rightarrow -\theta$. This is a direct consequence of the corresponding symmetry of the free energy with respect to such a transformation. However, in the presence of flexoelectric properties in the NLC, the symmetry of the $\theta(U)$ dependence with respect to the transformation $\theta \rightarrow -\theta$ is lost. This can be explained by the fact that when the sign of θ is changed, the curvature of the director profile is reversed. Consequently, the flexoelectric polarization vector also reverses its direction. As a result, the presence of flexoelectric polarization in one case leads to an increase in free energy, while in another case – on the contrary – to its decrease.

The flexoelectric coefficients e_1 and e_3 affect the $\theta(U)$ dependence in distinct ways. In order to illustrate this difference, we consider the approximation of small deformations of the director field near the initial homeotropic state by limiting ourselves to the linearized version of equation (4)

$$K_3 \theta''_{zz} + \frac{\epsilon_a \epsilon_\perp U^2}{4\pi \epsilon_\parallel d^2} \theta = 0, \quad (13)$$

with the boundary conditions (5), (6) for this equation

$$\left[K_3 \theta'_z - \frac{e_3 U}{d} - W \theta \right]_{z=0} = 0, \quad \theta|_{z=L} = 0. \quad (14)$$

For $e_3 = 0$ and $e_1 \neq 0$, the solution $\theta(U)$ of the linearized problem (13), (14) (see Fig. 2a) coincides with that in the absence of flexoelectric properties in the NLC. Therefore, in the case of $e_3 = 0$ (see Figs. 1, 2a), as the applied voltage U increases from zero, the orientational

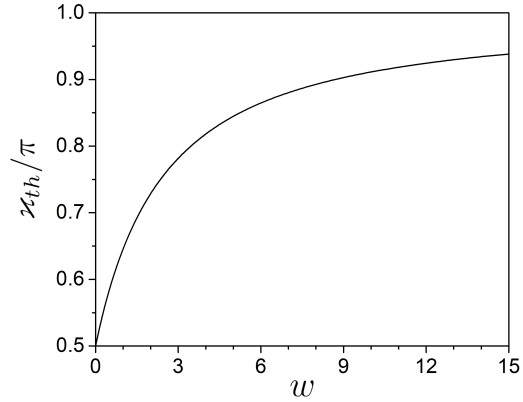


Figure 3. The dependence of the dimensionless threshold voltage κ_{th} on the dimensionless anchoring energy w .

transition of the system from the initial uniform homeotropic state to a non-uniform state has a threshold. The direction of the system's transition towards positive or negative angles θ is random and determined by fluctuations of the director field at the moment when the voltage U reaches its threshold value U_{th} . The threshold voltage U_{th} , found from the expressions (13), (14), is determined by the smallest positive root κ_{th} of the equation:

$$\tan \kappa = -\kappa/w, \quad (15)$$

where $\kappa = U \sqrt{\epsilon_a \epsilon_{\perp} L^2 / (4\pi \epsilon_{||} d^2 K_3)}$. The calculated dependence of the dimensionless threshold voltage κ_{th} on the anchoring energy w of the NLC with the substrate surface is shown in Fig. 3.

Non-zero values of the flexoelectric coefficient e_1 have little effect on the hysteresis parameters of the transition between the homeotropic and non-uniform states but lead to a significant change in both the width of the loop and the position of the hysteresis in the transition between the non-uniform and planar states. In particular, an increase in the absolute value of $|e_1|$ leads to an increase in the hysteresis width of the transition between the non-uniform and planar states and its shift toward lower voltage values when $\theta e_1 < 0$, and to a shift of the hysteresis toward higher voltage values and a decrease in its width, up to the disappearance of the hysteresis when $\theta e_1 > 0$. Overall, the impact of the flexoelectric coefficient e_1 on the director's stationary states becomes significant as the system moves away from the initial homeotropic configuration of the director.

The influence of the flexoelectric coefficient e_3 on the nature of the $\theta(U)$ dependence is most pronounced in the region of small director deviations from the initial homeotropic state (see Fig. 2b). In the case of $e_3 \neq 0$, the linearized equation (13) with respect to the angle θ becomes non-homogeneous, which corresponds to a thresholdless reorientation of the director from the initial homeotropic state to a non-uniform state as the applied voltage U increases from zero. As seen from (13), the symmetry of the system with respect to the transformation $\theta \rightarrow -\theta$ is broken. As a result, only one of the possible directions of the director's deviation ($\theta < 0$ or $\theta > 0$) from the initial homeotropic state is realized, depending on the sign of the flexoelectric coefficient e_3 . If $e_3 > 0$, then states with $\theta \leq 0$ are realized, while states with $\theta > 0$ cannot be reached by continuously varying the applied voltage. Conversely, for $e_3 < 0$, states with $\theta \geq 0$ are realized, while states with $\theta < 0$ are unattainable.

It should be noted that in both cases—small values of the flexoelectric coefficients e_1 and e_3 , as well as in the absence of flexoelectric properties in the NLC—the system's behavior is qualitatively similar. In particular, for small values of the flexoelectric coefficients and in the absence of flexoelectric properties in the NLC, the threshold voltages for the abrupt reorientation of the director from the uniform or weakly deformed homeotropic state to a significantly non-

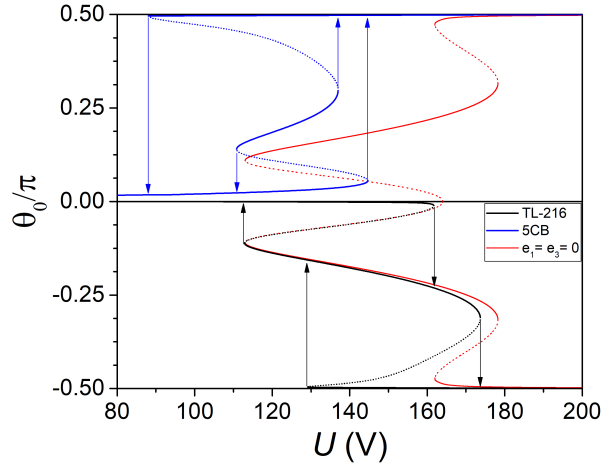


Figure 4. Dependence of the director surface angle θ_0 on the applied voltage U for the flexoelectric coefficients e_1 and e_3 corresponding to NLCs TL-216 (—), 5CB (—), and in the case of $e_1 = e_3 = 0$ (—).

uniform one differ by about 10 V (see Figs. 2a and 2b). At the same time, non-zero values of the flexoelectric coefficient e_3 , regardless of its sign, lead to a reduction in the threshold voltage for reorientation from the initial homeotropic state to a non-uniform one. An increase in the absolute value of $|e_3|$ leads to a decrease in the hysteresis width of the orientational transition between the non-uniform and planar states, as well as a shift of the hysteresis toward lower voltage values.

In Fig. 4, the dependence of the director surface angle θ_0 on the applied voltage U is shown for the flexoelectric coefficient values corresponding to the liquid crystals TL-216 ($e_1 = 0.000021 \text{ dyn}^{1/2}$, $e_3 = 0.000009 \text{ dyn}^{1/2}$) and 5CB ($e_1 = -0.00015 \text{ dyn}^{1/2}$, $e_3 = -0.00024 \text{ dyn}^{1/2}$)[61]. For comparison, the $\theta_0(U)$ dependence is also shown for the case where the NLC lacks flexoelectric properties. Overall, the contribution of non-zero values of both flexoelectric coefficients e_1 and e_3 to the dependence of the director angle on the voltage is qualitatively described by the combination of the previously analyzed contributions from each coefficient individually. Thus, the positive value of the e_3 coefficient for TL-216 and the negative value of e_3 for 5CB result in negative angles of director deviation from the initial homeotropic state being realized for TL-216, and only positive angles for 5CB. Since the signs of e_1 and e_3 coincide for both liquid crystals, the non-zero value of e_1 shifts the $\theta_0(U)$ curve towards lower voltage values in the region of large director deviations from the initial state $\theta = 0$. At the same time, the width and amplitude of the hysteresis in the orientational transition between the non-uniform and planar states increase.

The non-zero value of the coefficient e_3 shifts the $\theta_0(U)$ dependence toward lower voltage values and narrows the hysteresis width of the transition between the homeotropic and non-uniform states. It should be noted that for the 5CB NLC, with the chosen cell parameters, the shift in the hysteresis of orientational transitions between the weakly non-uniform homeotropic and non-uniform states, as well as between the planar and non-uniform states, is so pronounced that it causes an overlap of these hysteresis loops, forming a region of stable $\theta_0(U)$ solutions in the voltage range around $110 \div 140$ V. It is important to note that this region cannot be reached by the system as the applied voltage increases from zero. When the voltage reaches around 145 V (see Fig. 4), the system reorients from the uniform homeotropic state directly into the planar state, bypassing the non-uniform state. Similarly, this region of the $\theta_0(U)$ solution is also unreachable by decreasing the voltage from values above 150 V, since the solution transitions directly to the homeotropic state at $U \approx 87$ V. Overall, the contribution of non-zero flexoelectric coefficients is most significant in the regions of very small ($|\theta_0| \lesssim 0.02\pi$) and large ($|\theta_0| \gtrsim 0.2\pi$) director angles at the cell surface. This contribution becomes more pronounced as the absolute

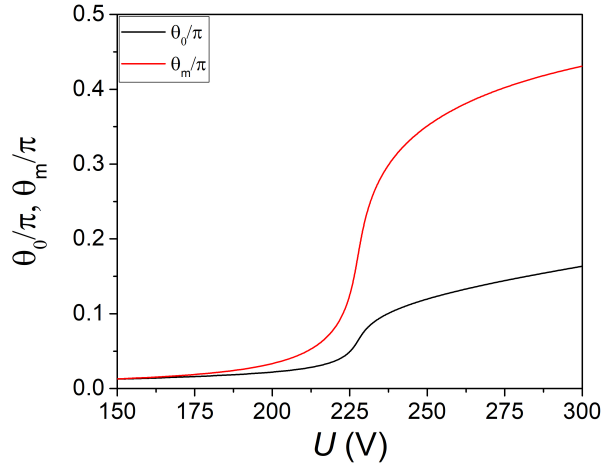


Figure 5. Dependence of the maximum director angle θ_m (—) and the surface director angle θ_0 (—) on the applied voltage U . $\epsilon_{\parallel} = 8$, $\epsilon_{\perp} = 5.17$, $e_1 = 0.0001 \text{ dyn}^{1/2}$, $e_3 = -0.0001 \text{ dyn}^{1/2}$.

values of the flexoelectric coefficients of the NLC increase.

It should be noted that there is also a possible case where the electrically induced orientational transition of the NLC director field from the homeotropic to the planar state occurs without any hysteresis. Such a transition is realized, for example, with a lower value of dielectric anisotropy in the NLC, as in [46]. In Fig. 5, the dependencies of the angles θ_m and θ_0 on the applied voltage U are shown for a significantly decreased value of the dielectric tensor's parallel component $\epsilon_{\parallel} = 8$. Due to the resulting reduction in dielectric anisotropy, the orientational transitions occur at higher voltage values and are not accompanied by hysteresis.

4. Regions of hysteresis existence

As calculations show, the number of hysteresis loops of the electro-induced orientational transition in the system and the regions of their existence are sensitive to small changes in the values of the parameters of the NLC cell, namely, the anchoring energy $w = WL/K_3$ of the latter with the surface, the elastic constant ratios $k = K_1/K_3$, and the values of the flexoelectric coefficients e_1 and e_3 of the NLC. Thus, in Fig. 6, diagrams of the number of hysteresis loops of the function $\theta(U)$ are presented depending on the magnitude of the ratio k of the elastic constants and the value of the anchoring energy w in the absence (Fig. 6a) and presence (Fig. 6b, c, d) of flexoelectric properties in the NLC. In the absence of flexoelectric properties in the NLC (Fig. 6a), the boundaries of the region of coexistence of two hysteresis loops are almost linear, $0.4 \lesssim k \lesssim 0.3w - 0.7$. Increasing the anchoring energy w leads to a rapid expansion of the region of existence of two hysteresis loops in terms of the parameter k values. For values $w \lesssim 0.3$, only one hysteresis loop can exist regardless of the value of the parameter k . It should be noted that Fig. 6a corresponds to director deviations both toward negative and positive values of the director angle θ due to the symmetry of the problem with respect to the transformation $\theta \rightarrow -\theta$.

Fig. 6b corresponds to director deviations toward negative values of the angle θ for the case of $e_1 = 0$, $e_3 = 0.0001 \text{ dyn}^{1/2}$. As the absolute value of the coefficient $|e_3|$ increases, the region of coexistence of two hysteresis loops, $0.6 \lesssim k \lesssim 0.3w - 0.8$, narrows with respect to the parameter k . At the same time, the boundaries of this region remain almost linear. It should be noted that the positive values of θ are not realized for $e_3 > 0$.

The presence of a non-zero value of the coefficient $e_1 = 0.0001 \text{ dyn}^{1/2}$ in the NLC (with $e_3 = 0$, $\theta > 0$, Fig. 6c) leads to a narrowing of the region of coexistence of two hysteresis loops, $1 \lesssim k \lesssim 0.3w - 0.5$, with respect to the parameter k for positive values of the angle θ , compared

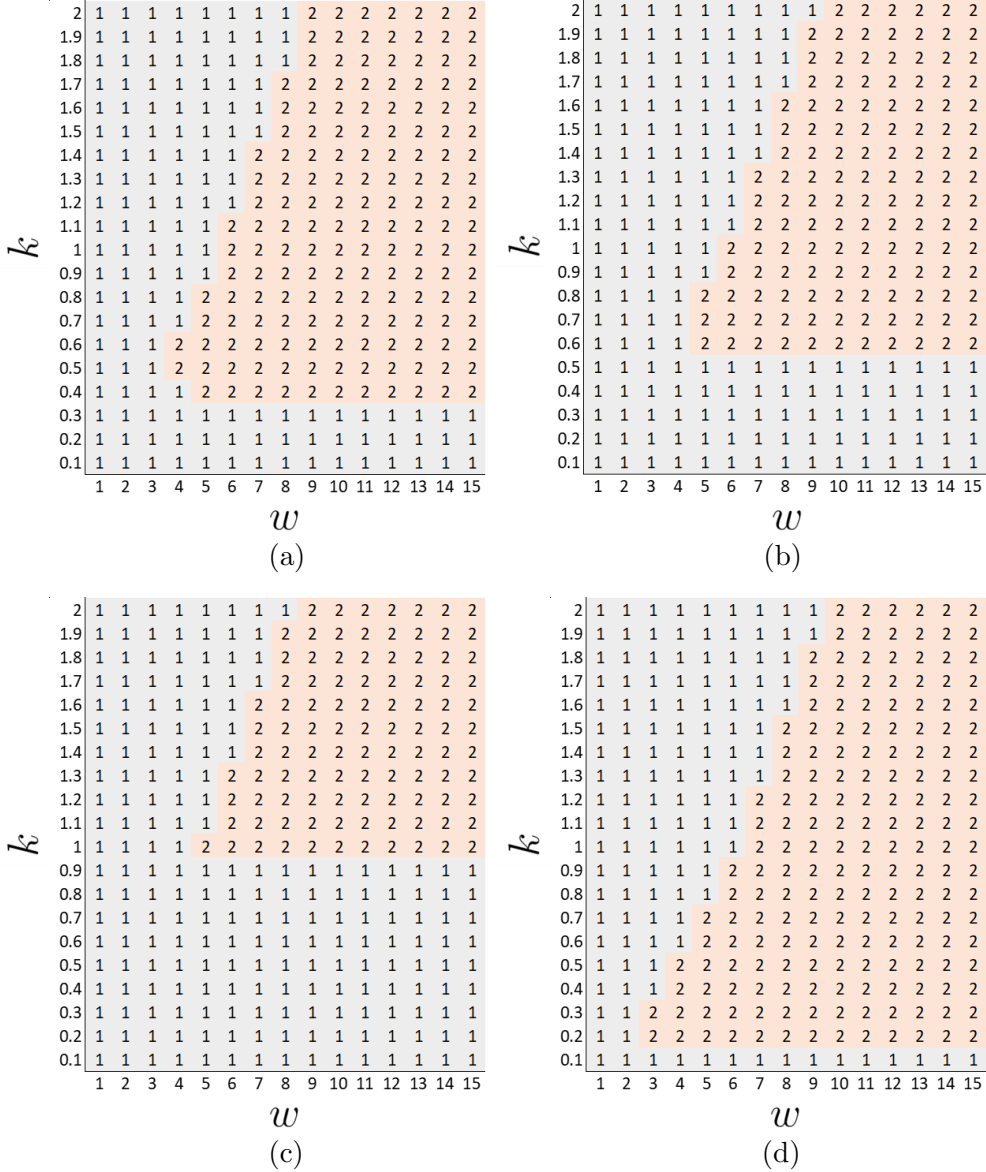


Figure 6. The number of hysteresis loops in the dependence $\theta_0(U)$ as a function of the anchoring energy magnitude w and the value of the parameter $k = K_1/K_3$. (a) $e_1 = e_3 = 0, \theta \geq 0$; (b) $e_1 = 0, e_3 = 0.0001 \text{ dyn}^{1/2}, \theta \leq 0$; (c) $e_1 = 0.0001 \text{ dyn}^{1/2}, e_3 = 0, \theta \geq 0$; (d) $e_1 = -0.0001 \text{ dyn}^{1/2}, e_3 = 0, \theta \geq 0$.

to the case $e_1 = e_3 = 0$. For negative values of θ or for negative values of the coefficient $e_1 = -0.0001 \text{ dyn}^{1/2}$ (these two cases are identical due to the symmetry of the problem with respect to the simultaneous change in the signs of the flexoelectric coefficients and the director angle), the corresponding region of coexistence of two hysteresis loops expands with respect to the parameter k , but shifts to smaller values compared to the case $e_1 = e_3 = 0$ (Fig. 6d).

In the case of non-zero values of both flexoelectric coefficients e_1 and e_3 , the overall picture in terms of the number of hysteresis loops in the system becomes significantly more complex. Coefficients e_1 and e_3 of opposite signs reduce the widths of the hysteresis loops of orientational transitions between the non-uniform and planar states, and between the homeotropic and non-uniform states, respectively, thus narrowing the region of parameter values k and w where two hysteresis loops exist. In the case of coefficients e_1 and e_3 having the same sign, the contribution of the coefficient e_1 is opposite to the contribution of e_3 in terms of the number of hysteresis loops, and such a problem requires separate investigation for specific values of e_1 and e_3 .

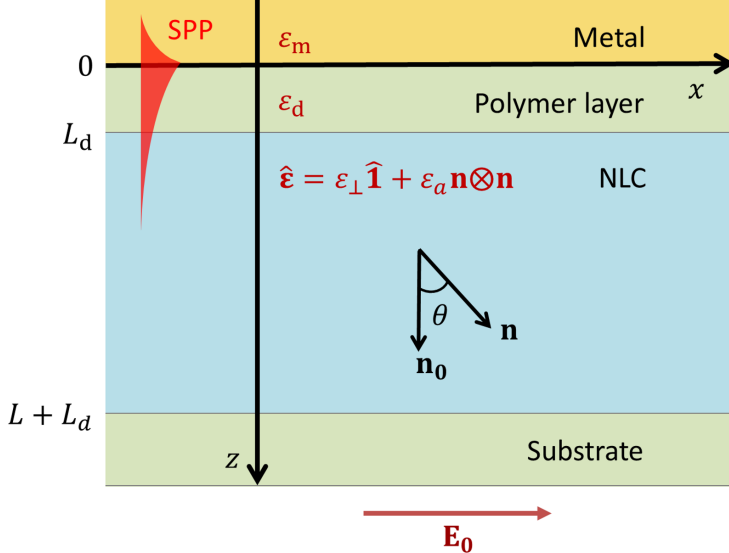


Figure 7. Structure of NLC – polymer layer – metal. Surface plasmon-polaritons can propagate at the polymer layer – metal interface.

5. Plasmon oscillations on the surface of the NLC cell

Let one of the polymer substrates of the cell with thickness L_d externally border with a metal layer. In such a system NLC – polymer – metal, under appropriate conditions, surface plasmon-polaritons (SPPs) can be excited at the polymer – metal interface. The propagation of SPPs in such a structure will be described in a Cartesian coordinate system, where the Oz axis is directed toward the NLC, and the xOy plane is aligned with the polymer-metal interface. The Ox axis is oriented in the direction of SPP propagation (see Fig. 7).

The electromagnetic field of the SPP will be considered as a monochromatic wave with frequency ω , $\mathbf{E}(\mathbf{r}, t) = \mathbf{E}(\mathbf{r})e^{-i\omega t}$, $\mathbf{H}(\mathbf{r}, t) = \mathbf{H}(\mathbf{r})e^{-i\omega t}$. If the polymer substrate is sufficiently thin, the electromagnetic field of the SPP will penetrate into the NLC and, accordingly, will be influenced by the director field distribution in the latter. The amplitudes of the electric and magnetic field oscillations of the SPP, due to its localized nature, decay exponentially as the distance from the polymer-metal interface increases. Therefore, the effect of the bounding substrate on the opposite side of the NLC layer on the SPP propagation parameters is negligibly small due to the exponential decay of the electromagnetic field. For the calculation of the SPP electromagnetic field, we will assume the NLC layer to be unbounded in the direction of the Oz axis. Thus, the SPP propagation medium is modeled as a three-layer system consisting of an isotropic homogeneous polymer layer, bounded on both sides by semi-infinite metal and NLC layers. To account for the influence of the anisotropy and inhomogeneity of the NLC on the SPP propagation, we will use perturbation theory [43,46]. In the zero-order approximation of this theory, the electric $\mathbf{E}(\mathbf{r})$ and magnetic $\mathbf{H}(\mathbf{r})$ field vectors of the SPP are solutions of the Maxwell equations in a homogeneous isotropic medium with dielectric permittivity.

$$\varepsilon_0(z) = \varepsilon_m \chi(-z) + \varepsilon_d \chi(z), \quad (16)$$

where ε_m , ε_d are the dielectric permittivities of the metal and the polymer, respectively, at the frequency ω of SPP propagation. Here, $\chi(t)$ is the Heaviside function: $\chi(t) = 0$ for $t < 0$ and $\chi(t) = 1$ for $t > 0$. The electric and magnetic field vectors of the SPP, found in the zero-order perturbation theory within the isotropic approximation, have the following form:

$$\begin{aligned} \mathbf{E}_0(x, z) &= \frac{cA}{\omega \varepsilon_{m,d}} (\pm ik_{m,d}, 0, -k_0) e^{ixk_0 \mp zk_{m,d}}, \\ \mathbf{H}_0(x, z) &= A(0, 1, 0) e^{ixk_0 \mp zk_{m,d}}, \end{aligned} \quad (17)$$

where A is the amplitude factor, and the indices m and d denote the media of the metal ($z < 0$) and polymer ($z > 0$), respectively. The propagation constants k_0 and $k_{m,d}$ are expressed through the dielectric permittivities of the metal ε_m and the polymer ε_d as follows:

$$k_0 = \frac{\omega}{c} \sqrt{\frac{\varepsilon_d \varepsilon_m}{\varepsilon_d + \varepsilon_m}}, \quad k_{m,d} = \frac{\omega}{c} \sqrt{-\frac{\varepsilon_{m,d}^2}{\varepsilon_d + \varepsilon_m}}. \quad (18)$$

The anisotropy and inhomogeneity of the NLC are taken into account as a perturbation of the zero-order approximation (17). To do this, we express the dielectric permittivity of the three-layer structure in the following form:

$$\hat{\varepsilon}(z) = \varepsilon_0(z) \hat{\mathbf{1}} + \eta (\varepsilon_c \mathbf{1} + \varepsilon_a \mathbf{n} \otimes \mathbf{n}) \chi(z - L_d), \quad \eta \ll 1, \quad (19)$$

where $\varepsilon_a = \varepsilon_{\parallel} - \varepsilon_{\perp}$, $\varepsilon_c = \varepsilon_{\perp} - \varepsilon_d$, where ε_{\parallel} and ε_{\perp} are the components of the dielectric permittivity tensor of the homogeneous NLC parallel and perpendicular to the director, respectively, at the frequency ω .

The solution of the system of Maxwell's equations in a medium with the dielectric permittivity tensor $\hat{\varepsilon}(z)$ (19) is sought for the electric and magnetic field vectors of the SPP as an expansion in terms of the small parameter η :

$$\begin{aligned} \mathbf{E} &= \mathbf{E}_0 + \eta \mathbf{E}_1 + o(\eta), \\ \mathbf{H} &= \mathbf{H}_0 + \eta \mathbf{H}_1 + o(\eta), \end{aligned} \quad (20)$$

where the corrections \mathbf{E}_1 and \mathbf{H}_1 account for the anisotropy and inhomogeneity of the NLC layer. Solving the equations for \mathbf{E}_1 and \mathbf{H}_1 , in the linear approximation with respect to η , we find the correction to the zero-order approximation $n_{eff}^0 = ck_0/\omega$ of the effective refractive index of the SPP. As a result, the latter takes the form

$$n_{eff} = \frac{ck_0}{\omega} (1 + Ne^{-2k_d L_d}), \quad (21)$$

where

$$\begin{aligned} N = & \frac{\varepsilon_m \varepsilon_c}{2(\varepsilon_d + \varepsilon_m) \varepsilon_d} - \frac{(\varepsilon_d + 2\varepsilon_m) \varepsilon_m \varepsilon_a}{6\varepsilon_d (\varepsilon_d^2 - \varepsilon_m^2)} + \frac{\varepsilon_m \varepsilon_a}{2\varepsilon_d (\varepsilon_d - \varepsilon_m)} - \\ & - \frac{\varepsilon_m \varepsilon_a k_d e^{2k_d L_d}}{\varepsilon_d (\varepsilon_d - \varepsilon_m)} \int_{L_d}^{\infty} \sin^2 \theta(z - L_d) e^{-2k_d z} dz. \end{aligned} \quad (22)$$

Expression (21) gives the value of the effective refractive index of the SPP for an arbitrary director profile in the volume of the NLC.

In Fig. 8, the dependence of the effective refractive index n_{eff} of the SPP on the applied voltage U is shown for the case where gold is used as the metal. The calculations were performed in the optical range at a wavelength of $\lambda = 800$ nm for the following values of the dielectric constants of gold, the polymer, and the liquid crystal mixture E7: $\varepsilon_m = -26.43$, $\varepsilon_d = 2.81$, $\varepsilon_{\parallel} = n_e^2 = 2.92$, $\varepsilon_{\perp} = n_o^2 = 2.28$, which were obtained using interpolation formulas [44,62]. Regardless of the values of the flexoelectric coefficients of the NLC, the dependence $n_{eff}(U)$ is a piecewise continuous decreasing function. The regions of continuous variation of n_{eff} are bounded by discontinuity points associated with the abrupt reorientation of the director as the voltage U changes.

In the case of $e_1 = e_3 = 0$, the NLC is oriented almost homeotropically throughout the entire thickness of the cell, as long as the applied voltage U does not exceed the threshold value of the orientational instability, $U_{th1} \approx 165$ V. Therefore, the refractive index of the SPP propagating

along the surface of the cell is approximately $n_{eff} \approx 1.78$ and remains almost independent of U within this range (see Fig. 8). As the voltage increases and reaches the threshold value U_{th1} , an abrupt orientational transition occurs in the system, where the director field switches from a uniform homeotropic state to a significantly non-uniform one. As a result, the effective refractive index of the SPP decreases abruptly. With a further increase in voltage within the range of approximately $165 \div 180$ V, the effective refractive index of the SPP gradually decreases while the non-uniform director profile remains stable. Another abrupt decrease in the effective refractive index occurs when the voltage reaches the second threshold value $U_{th2} \approx 180$ V. At this point, the director field in the NLC volume abruptly reorients to a planar state. When the voltage decreases from values higher than U_{th2} , the reverse abrupt changes in the effective refractive index of the SPP occur at lower threshold voltages $U'_{th} < U_{th}$. This indicates the presence of hysteresis in the value of n_{eff} as the voltage U changes. The presence of two hysteresis loops in the dependence of $n_{eff}(U)$ is a direct consequence of the two hysteresis loops in the orientational restructuring of the NLC director field as the voltage changes (see Figs. 1, 2). The magnitude of the change in n_{eff} within both hysteresis loops is primarily determined by the magnitude of the change in the director orientation angle near the surface where the SPP is excited. For $e_3 \neq 0$, the orientational transitions from the initial homeotropic state to the significantly non-uniform state are threshold-free, meaning that an arbitrary increase in the applied voltage results in a decrease of the effective index n_{eff} . However, for the voltages $U \lesssim 110$ V and $U \gtrsim 180$ V, the dependence $n_{eff}(U)$ is almost constant, therefore the range of voltage values at which the dependence $n_{eff}(U)$ is sensitive to the applied voltage U is limited to approximately $110 \div 180$ V. Non-zero values of the flexoelectric coefficient e_3 shift the $n_{eff}(U)$ dependence toward lower voltage values, regardless of the sign of the coefficient (see Fig. 8a). At the same time, the voltage range where the $n_{eff}(U)$ dependence is not constant narrows from $110 \div 180$ V to approximately $110 \div 170$ V.

In the case of $e_1 \neq 0$ but $e_3 = 0$, the dependence $n_{eff}(U)$ has two possible branches corresponding to the deviations of the director toward positive and negative values of the angles θ (see Fig. 8b). The solution that is realized when the initial homeotropic state of the NLC loses stability ($U_{th1} \approx 165$ V) is determined by the fluctuations of the director. If the director deviates toward positive values of the angles θ , the $n_{eff}(U)$ dependence shifts toward higher voltage values U , while for negative values of θ , this dependence shifts toward lower values of U compared to the case of $e_1 = e_3 = 0$.

It should be noted that the presence of flexoelectric properties in the NLC does not affect the range Δn_{eff} of possible variations in the values of the effective refractive index. This range is obtained by substituting the solutions $\theta = 0$ at $U = 0$ and $|\theta| \approx \pi/2$ at $U \rightarrow \infty$ into relation (21):

$$\Delta n_{eff} = \sqrt{\frac{\varepsilon_d \varepsilon_m}{\varepsilon_d + \varepsilon_m}} \frac{|\varepsilon_m| \varepsilon_a}{\varepsilon_d (\varepsilon_d - \varepsilon_m)} \exp\left(-\frac{2\omega \varepsilon_d L_d}{c |\varepsilon_d + \varepsilon_m|}\right). \quad (23)$$

In general, an increase in the voltage U leads to a decrease in the effective refractive index n_{eff} of the SPP, which can be explained as follows. As the voltage U increases from zero, an orientational transition of the director field from the homeotropic to the planar state occurs within the NLC volume. Since the \mathbf{E} vector of the electric field of the SPP predominantly oscillates along the Oz axis, the refractive index of the NLC experienced by the SPP changes from n_e to n_o . This results in a decrease in the n_{eff} of the SPP.

In Fig. 9, the dependencies of the effective refractive index n_{eff} of the SPP on the voltage U are shown for flexoelectric coefficients corresponding to the liquid crystals TL-216 and 5CB. An increase in the absolute values of coefficients e_1 and e_3 shifts the orientational transitions toward lower voltage values of U . The width of the hysteresis loop bounded by transitions 1 and 1' decreases, while the hysteresis loop bounded by transitions 2 and 2' increases (see Fig. 9). For the NLC 5CB, with the applied cell parameters, these changes result in an overlap of the hysteresis loops of the orientational transitions between the homeotropic and non-uniform states and between the planar and non-uniform states. As a result, the stable solution with n_{eff} values

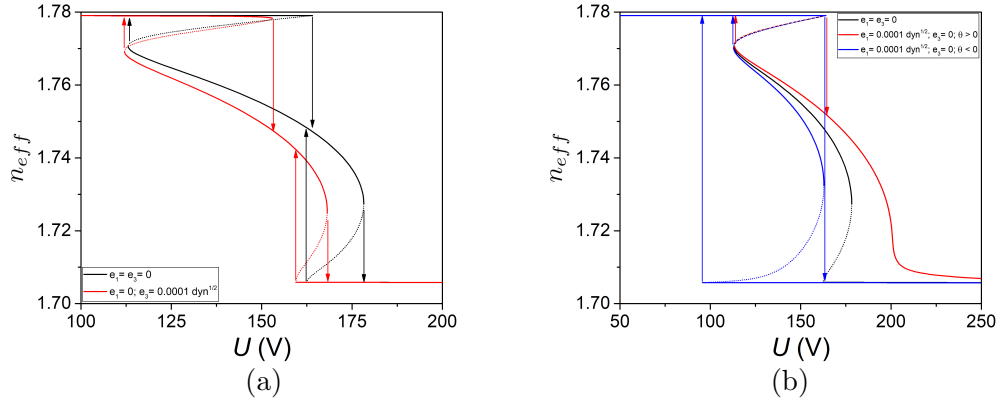


Figure 8. Dependence of the effective refractive index n_{eff} of the SPP on the voltage U . $L_d = 100 \text{ nm}$, $\lambda = 800 \text{ nm}$, $e_1 = e_3 = 0$ (—). (a) $e_3 = 0.0001 \text{ dyn}^{1/2}$, $e_1 = 0$ (—); (b) $e_1 = 0.0001 \text{ dyn}^{1/2}$, $e_3 = 0$, $\theta > 0$ (—), $\theta < 0$ (—).

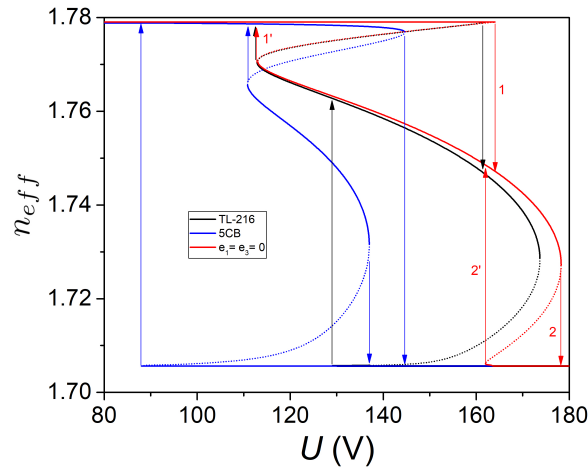


Figure 9. Dependence of n_{eff} on the voltage U for flexoelectric coefficients corresponding to the NLCs TL-216 (—), 5CB (—), and for the case of $e_1 = e_3 = 0$ (—). $L_d = 100 \text{ nm}$, $\lambda = 800 \text{ nm}$.

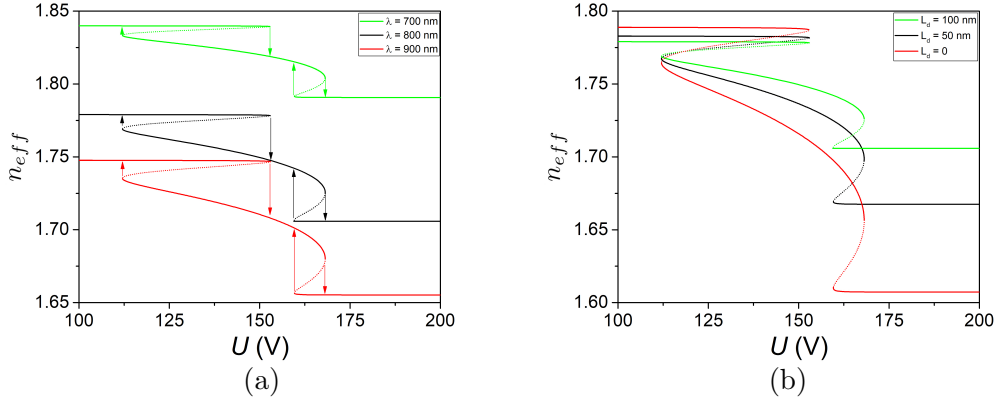


Figure 10. Dependence of the effective refractive index n_{eff} on the voltage U for different wavelengths λ (a) and polymer film thicknesses L_d (b). $e_1 = 0$, $e_3 = 0.0001 \text{ dyn}^{1/2}$.

approximately ranging from 1.735 to 1.765 becomes inaccessible through either increasing or decreasing the voltage U .

In Fig. 10a, the dependencies of the effective refractive index on the voltage for various SPP wavelengths λ are shown. Changing the values of λ does not alter the hysteresis transition voltages but does affect both the magnitude of n_{eff} and its range of variation Δn_{eff} . Specifically, increasing the wavelength λ leads to a decrease in n_{eff} and an expansion of the range of Δn_{eff} values.

The dependence of the SPP refractive index on the applied voltage for different polymer film thicknesses L_d is shown in Fig. 10b. An increase in the thickness L_d results in a narrowing of the range of variation Δn_{eff} of the SPP effective refractive index with changing voltage. Calculations indicate that the threshold voltages at which hysteresis transitions occur do not depend on the thickness L_d of the polymer film.

If the refractive index n_d of the polymer film lies within the range of the NLC refractive index, specifically $n_o \leq n_d \leq n_e$, there exists a director field configuration in the cell volume where the effective refractive index of the near-surface NLC layer approximates n_d . In this case, the system's dependence on the thickness L_d of the polymer film vanishes. In Fig. 10b, this scenario corresponds to the point ($U \approx 120 \text{ V}$, $n_{eff} \approx 1.77$), where curves for different polymer film thicknesses converge. For the given system parameters, this specific point corresponds to an unstable solution and therefore will not be realized. However, for NLCs with slightly different dielectric constants, a similar lack of dependence on the polymer film thickness L_d may occur for a stable director field configuration.

6. Discussion and Conclusions

In the plane deformation approximation, the electro-induced orientational instability of the director in a cell of homeotropically oriented flexoelectric NLC has been theoretically investigated. It has been established that the orientational transitions of the director field between the initial homeotropic and non-uniform states, as well as between the non-uniform and planar states, during the increase/decrease of the applied voltage U , may be accompanied by one or two hysteresis loops, or may occur without hysteresis at all. The influence of the applied voltage U and the cell parameters on these orientational transitions has been studied, specifically, the anchoring energy $w = WL/K_3$ of the NLC with the surface, the elastic constant ratio $k = K_1/K_3$ of the NLC, and the flexoelectric coefficients e_1 and e_3 of the NLC.

For zero values of the flexoelectric coefficient e_3 of the NLC, but with $e_1 \neq 0$, the orientational transition of the system from the initial uniform homeotropic state to a non-uniform one has a threshold for any anchoring energy w as the voltage U increases from zero. When the voltage reaches the threshold value U_{th} , the direction of the director deviation, whether toward positive

or negative values of the angle θ , is random and determined solely by fluctuations in the director field. Conversely, in the case where $e_1 = 0$ but $e_3 \neq 0$, the reorientation of the NLC from the initial uniform homeotropic state to a non-uniform one occurs without a threshold as the voltage increases from zero. In this case, only one direction of the director deviation is realized—either toward positive or negative values of the angle θ . The sign of θ is determined by the sign of the flexoelectric coefficient e_3 , $\text{sign}(\theta) = -\text{sign}(e_3)$. This is a consequence of the symmetry breaking of the problem with respect to the substitution $\theta \rightarrow -\theta$, which occurs near the initial homeotropic state.

Non-zero values of the coefficient e_1 shift the voltage dependence $\theta(U)$ of the director angle toward higher values of U when $\theta e_1 > 0$ and toward lower values of U in the opposite case, $\theta e_1 < 0$. In this case, the width and amplitude of the hysteresis of the orientational transition between the non-uniform and planar states increase, while the hysteresis parameters of the transition between the non-uniform and homeotropic states remain largely unchanged. Meanwhile, a non-zero value of the flexoelectric coefficient e_3 shifts the dependence $\theta(U)$ toward lower voltages and narrows the hysteresis width of the transition between the homeotropic and non-uniform states, with little impact on the hysteresis parameters of the transition between the planar and non-uniform states. Increasing the absolute value of the coefficient $|e_3|$ and the magnitude of $e_1 \text{sign}(e_3)$ in the NLC reduces the threshold voltages for the abrupt reorientation of the director compared to the case without flexoelectric properties in the NLC. In general, when both coefficients e_1 and e_3 are non-zero, their contributions to the dependence $\theta(U)$ are qualitatively described by a combination of the contributions from each coefficient individually.

The influence of cell parameter values, particularly the flexoelectric coefficients of the NLC, on the number of hysteresis transitions in the electro-induced orientational instability of the director has been studied. Regardless of the presence of flexoelectric properties in the NLC, both orientational transitions between the homeotropic and non-uniform states, as well as between the non-uniform and planar states, are accompanied by hysteresis within the parameter range $k_{th2}(w) < k < k_{th1}(w)$ (where $k_{th2} < k_{th1}$). This “double” hysteresis region expands with increasing values of the anchoring energy w . Outside of this region, only one hysteresis loop of the director field’s orientational restructuring is realized in the system. Specifically, a single hysteresis loop occurs for all values of the parameter k and for anchoring energies w below a certain critical value w_{th} , determined by the condition $k_{th2}(w) = k_{th1}(w)$. Increasing the absolute value $|e_3|$ and decreasing the magnitude of $e_1 \text{sign}(e_3)$ narrow the parameter ranges of k and w for which both hysteresis loops of the orientational transitions between the homeotropic and non-uniform states, and between the planar and non-uniform states, exist, compared to the case where flexoelectric properties in the NLC are absent ($e_1 = e_3 = 0$).

The influence of an external electric field on the propagation conditions and parameter values of the surface plasmon-polariton in an NLC – polymer – metal system has been studied. The effective refractive index n_{eff} of the SPP has been calculated, and its dependence on the applied voltage U , the polymer film thickness L_d , and the NLC layer parameters, specifically the flexoelectric coefficients e_1 and e_3 , has been investigated. Changes in the effective refractive index n_{eff} of the SPP, caused by varying the voltage, may also be accompanied by one or two hysteresis loops, resulting from the hysteresis in the dependence $\theta(U)$. It has been established that n_{eff} increases with higher values of the NLC surface anchoring energy and decreases with lower voltage and wavelength values.

Increasing the absolute value of the coefficient $|e_3|$ shifts the $n_{eff}(U)$ dependence toward lower voltage values and narrows the voltage range U over which the $n_{eff}(U)$ dependence is not constant. Increasing the value of e_1 shifts the $n_{eff}(U)$ dependence toward higher voltages U when $e_3 < 0$, and toward lower values of U when $e_3 > 0$.

It should be noted that the range of variation in the SPP refractive index n_{eff} expands with a decrease in the polymer film thickness and an increase in wavelength. The thinner the polymer film and the longer the wavelength, the higher the values that n_{eff} of the SPP can achieve. If the refractive index n_d of the polymer film lies within the range of the NLC refractive index, $n_o \leq n_d \leq n_e$, the dependence of n_{eff} on the polymer film thickness may disappear. This occurs within the range of voltage values U where the effective refractive index of the near-surface NLC

layer is close to n_d .

Disclosure statement

The authors declare no conflict of interest.

Funding

The authors have received no external funding.

References

- [1] Khoo IC. Liquid crystals. John Wiley & Sons; 2022.
- [2] Kato T, Uchida J, Ichikawa T, et al. Functional liquid crystals towards the next generation of materials. *Angewandte Chemie International Edition*. 2018;57(16):4355–4371.
- [3] Sato S. Applications of liquid crystals to variable-focusing lenses. *Optical Review*. 1999;6:471–485.
- [4] Schadt M. Liquid crystal materials and liquid crystal displays. *Annual review of materials science*. 1997;27(1):305–379.
- [5] De Gennes PG, Prost J. The physics of liquid crystals. Oxford university press; 1993. 83.
- [6] Lagerwall JP, Scalia G. A new era for liquid crystal research: Applications of liquid crystals in soft matter nano-, bio-and microtechnology. *Current Applied Physics*. 2012;12(6):1387–1412.
- [7] Castellano JA. Surface anchoring of liquid crystal molecules on various substrates. *Molecular crystals and liquid crystals*. 1983;94(1-2):33–41.
- [8] Yakovkin I, Lesiuk A, Ledney M, et al. Director orientational instability in a planar flexoelectric nematic cell with easy axis gliding. *Journal of Molecular Liquids*. 2022;363:119888.
- [9] Tarnavskyy O, Ledney M. Orientational instability of the director in a nematic cell caused by electro-induced anchoring modification. *Condensed Matter Physics*. 2021;24(1):13601.
- [10] Ellison A, Cornejo IA. Glass substrates for liquid crystal displays. *International Journal of Applied Glass Science*. 2010;1(1):87–103.
- [11] Tarnavskyy O, Savchenko A, Ledney M. Two-dimensional director configurations in a nematic-filled cylindrical capillary with the hybrid director alignment on its surface. *Liquid Crystals*. 2020;47(6):851–858.
- [12] Tarnavskyy O, Ledney M. Equilibrium locations of defects in two-dimensional configurations of the nlc director field. *Liquid Crystals*. 2023;50(1):21–35.
- [13] Lesiuk A, Ledney M, Tarnavskyy O. Orientational instability of nematic liquid crystal in a homeotropic cell with boundary conditions controlled by an electric field. *Liquid Crystals*. 2019;46(3):469–483.
- [14] Lesiuk A, Ledney M, Tarnavskyy O. Orientational instability induced by the electric field in a cell of a nematic liquid crystal with negative dielectric anisotropy. *Ukrainian journal of physics*. 2017;62(9):779–779.
- [15] Zel'dovich BY, Tabiryan N, Chilingaryan YS. Freedericksz transitions induced by light fields. *Sov Phys JETP*. 1981;54(1):32–37.
- [16] Durbin S, Arakelian S, Shen Y. Optical-field-induced birefringence and freedericksz transition in a nematic liquid crystal. *Physical Review Letters*. 1981;47(19):1411.
- [17] Zolot'Ko A, Kitaeva V, Kroo N, et al. The effect of an optical field on the nematic phase of the liquid crystal ocbp. *Jetp Lett*. 1980;32(2):158–162.
- [18] Brasselet E, Lherbier A, Dubee LJ. Transverse nonlocal effects in optical reorientation of nematic liquid crystals. *JOSA B*. 2006;23(1):36–44.
- [19] Ledney M, Pinkevych I. Influence of anchoring at a nematic cell surface on threshold spatially periodic reorientation of a director. *Liquid Crystals*. 2007;34(5):577–583.
- [20] Lesiuk A, Ledney M, Tarnavskyy O, et al. Electro-optical effect in a planar nematic cell with electric field sensitive boundary conditions. *Molecular Crystals and Liquid Crystals*. 2017;647(1):320–328.
- [21] Ong HL. Optically induced freedericksz transition and bistability in a nematic liquid crystal. *Physical Review A*. 1983;28(4):2393.

- [22] Vella A, Piccirillo B, Santamato E. Coupled-mode approach to the nonlinear dynamics induced by an elliptically polarized laser field in liquid crystals at normal incidence. *Physical Review E*. 2002; 65(3):031706.
- [23] Brasselet E, Piccirillo B, Santamato E. Three-dimensional model for light-induced chaotic rotations in liquid crystals under spin and orbital angular momentum transfer processes. *Physical Review E*. 2008;78(3):031703.
- [24] Budagovsky I, Pavlov D, Shvetsov S, et al. First-order light-induced orientation transition in nematic liquid crystal in the presence of low-frequency electric field. *Applied Physics Letters*. 2012;101(2).
- [25] D'Alessandro G, Wheeler AA. Bistability of liquid crystal microcavities. *Physical Review A*. 2003; 67(2):023816.
- [26] Ilyina V, Cox S, Sluckin T. A computational approach to the optical freedericksz transition. *Optics communications*. 2006;260(2):474–480.
- [27] Frisken B, Palffy-Muhoray P. Electric-field-induced twist and bend freedericksz transitions in nematic liquid crystals. *Physical Review A*. 1989;39(3):1513.
- [28] Ledney MF, Tarnavskyy OS. Influence of the anchoring energy on hysteresis at the freedericksz transition in confined light beams in a nematic cell. *Liquid Crystals*. 2012;39(12):1482–1490.
- [29] Ledney M, Tarnavskyy O, Khimich V. Influence of dc electric field on the hysteresis of light-induced freedericksz transition in a nematic cell. *Ukrainian journal of physics*. 2016;61(2):117–117.
- [30] Laudyn UA, Miroshnichenko AE, Krolkowski W, et al. Observation of light-induced reorientational effects in periodic structures with planar nematic-liquid-crystal defects. *Applied Physics Letters*. 2008;92(20).
- [31] Miroshnichenko AE, Brasselet E, Kivshar YS. Light-induced orientational effects in periodic photonic structures with pure and dye-doped nematic liquid crystal defects. *Physical Review A*. 2008; 78(5):053823.
- [32] Ledney M, Tarnavskyy O, Lesiuk A, et al. Interaction of electromagnetic waves in nematic waveguide. *Molecular Crystals and Liquid Crystals*. 2016;638(1):1–16.
- [33] Meyer RB. Piezoelectric effects in liquid crystals. *Physical Review Letters*. 1969;22(18):918.
- [34] Wu WT. Liquid crystal pretilt angle control. mechanism, electro-optical properties and numerical analysis [dissertation]. Sl: sn; 2016.
- [35] Kim MS, Bos PJ, Kim DW, et al. Flexoelectric effect in an in-plane switching (ips) liquid crystal cell for low-power consumption display devices. *Scientific reports*. 2016;6(1):35254.
- [36] Skarabot M, Mottram NJ, Kaur S, et al. Flexoelectric polarization in a nematic liquid crystal enhanced by dopants with different molecular shape polarities. *ACS omega*. 2022;7(11):9785–9795.
- [37] Sprokel G, Santo R, Swalen J. Determination of the surface tilt angle by attenuated total reflection. *Molecular Crystals and Liquid Crystals*. 1981;68(1):29–38.
- [38] Sprokel G. The reflectivity of a liquid crystal cell in a surface plasmon experiment. *Molecular Crystals and Liquid Crystals*. 1981;68(1):39–45.
- [39] Welford K, Sambles J. Detection of surface director reorientation in a nematic liquid crystal. *Applied physics letters*. 1987;50(14):871–873.
- [40] Welford K, Sambles J, Clark M. Guided modes and surface plasmon-polaritons observed with a nematic liquid crystal using attenuated total reflection. *Liquid Crystals*. 1987;2(1):91–105.
- [41] Lesiuk A, Ledney M, Reshetnyak VY. Light-induced fredericks transition in the nematic liquid crystal cell with plasmonic nanoparticles at a cell bounding substrate. *Physical Review E*. 2022; 106(2):024706.
- [42] Daly KR. Light-matter interaction in liquid crystal cells [dissertation]. University of Southampton; 2011.
- [43] Daly KR, Abbott S, D'Alessandro G, et al. Theory of hybrid photorefractive plasmonic liquid crystal cells. *JOSA B*. 2011;28(8):1874–1881.
- [44] Abbott SB. Energy transfer between surface plasmon polariton modes with hybrid photorefractive liquid crystal cells [dissertation]. University of Southampton; 2012.
- [45] Abbott SB, Daly KR, D'Alessandro G, et al. Photorefractive control of surface plasmon polaritons in a hybrid liquid crystal cell. *Optics Letters*. 2012;37(13):2436–2438.
- [46] Yakovkin I, Ledney M. Electrically induced orientational instability of the director in a homeotropic nematic liquid crystal cell and its effect on surface plasmon oscillations. *Phase Transitions*. 2023; :1–11.
- [47] Yakovkin I, Ledney M. Electrocontrol over surface plasmon oscillations in a homeotropic nematic liquid crystal cell. *Ukrainian journal of physics*. 2024;69(6):417–430.
- [48] Caldwell ME, Yeatman EM. Surface-plasmon spatial light modulators based on liquid crystal. Ap-

- plied optics. 1992;31(20):3880–3891.
- [49] Bortolozzo U, Residori S, Huignard J. Beam coupling in photorefractive liquid crystal light valves. *Journal of Physics D: Applied Physics*. 2008;41(22):224007.
 - [50] Yang F, Sambles J. Microwave liquid crystal wavelength selector. *Applied Physics Letters*. 2001; 79(22):3717–3719.
 - [51] Wang Y. Voltage-induced color-selective absorption with surface plasmons. *Applied Physics Letters*. 1995;67(19):2759–2761.
 - [52] Wang Y, Russell SD, Shimabukuro RL. Voltage-induced broad-spectrum reflectivity change with surface-plasmon waves. *Journal of applied physics*. 2005;97(2).
 - [53] Buchnev O, Dyadyusha A, Kaczmarek M, et al. Enhanced two-beam coupling in colloids of ferroelectric nanoparticles in liquid crystals. *JOSA B*. 2007;24(7):1512–1516.
 - [54] Cook G, Glushchenko A, Reshetnyak V, et al. Nanoparticle doped organic-inorganic hybrid photorefractives. *Optics express*. 2008;16(6):4015–4022.
 - [55] Dickson W, Wurtz GA, Evans PR, et al. Electronically controlled surface plasmon dispersion and optical transmission through metallic hole arrays using liquid crystal. *Nano letters*. 2008;8(1):281–286.
 - [56] Rapini A, Papoular M. Distorsion dune lamelle nematicque sous champ magnetique conditions dancrage aux parois. *Le Journal de Physique Colloques*. 1969;30(C4):C4–54.
 - [57] Romanov V, Sklyarenko G. Threshold effects in homeotropically oriented nematic liquid crystals in an external electric field. *Journal of Experimental and Theoretical Physics*. 1999;89:288–291.
 - [58] Blinov LM, Chigrinov VG. Electrooptic effects in liquid crystal materials. Springer Science & Business Media; 2012.
 - [59] Chao PP, Kao YY, Hsu CJ. A new negative liquid crystal lens with multiple ring electrodes in unequal widths. *IEEE photonics journal*. 2012;4(1):250–266.
 - [60] Warlimont H, Martienssen W. Springer handbook of materials data. Springer; 2018.
 - [61] Buka A, Éber N. Flexoelectricity in liquid crystals: theory, experiments and applications. World Scientific; 2012.
 - [62] Tkachenko V, Abbate G, Marino A, et al. Nematic liquid crystal optical dispersion in the visible-near infrared range. *Molecular Crystals and Liquid Crystals*. 2006;454(1):263–665.